The Use of Weber Number to Predict Morphology in the Electrospinning of Poly(ethylene oxide) Nanofibers

Christopher C. Call, Christian J. Schwartz

Department of Mechanical Engineering, Texas A&M University, College Station, Texas 77843

Received 9 June 2010; accepted 9 August 2010
DOI 10.1002/app.33201
Published online 5 November 2010 in Wiley Online Library (wileyonlinelibrary.com).

ABSTRACT: In the electrospinning of polymer nanofibers, an electrically driven jet of polymer solution travels to a grounded target to be collected. The morphology of the resulting nanofibers can be manipulated through process parameters, though little work has been done to correlate electrospinning parameters with those of the free-jet flow of pure liquids. This is essential when the nanofibers hold entrained beaded structures indicative of jet breakup. The effects of applied voltage and solution concentration on the fiber morphology of electrospun aqueous solutions of poly(ethylene oxide) were investigated. Solution concentrations of 4–8 wt % were used along with voltages of 4.5–11 kV to produce nanofibers with and without entrained beads. It was determined that the calculated Weber number for each condition correlated well with the resulting morphology. These results may suggest that Weber number may also be used to predict nanofibers morphology in the electrospinning of other polymer systems. © 2010 Wiley Periodicals, Inc. J Appl Polym Sci 120: 880–885, 2011

Key words: nanofiber; water-soluble polymers; processing

INTRODUCTION

Electrospinning is one of a few processes that have the capability to produce nanofibers. Electrospinning has potential in biomedical applications,[1] fuel cells,[2] filtration,[3] and composites.[4] In biomedical applications, electrospinning can be used to control drug delivery rates that control therapeutic effects, convenience, and toxicity.[1] In filtration, electrospun mats can filter particles in the submicron range.[3] Both polymer and ceramic nanofibers can be electrospun to create fibers with diameters ranging from tens of nanometers to several microns.

Electrospinning is the electrically driven drawing of a polymer solution into a viscoelastic polymer jet that ultimately produces a mat of solid polymer fibers. In practical terms, the basic components of an electrospinning system include a high-voltage power supply, a polymer dissolved in solution, a chamber with a conductive nozzle to hold the solution, and a grounded collection plate that is separated from the nozzle by a chosen distance. By applying sufficient electric potential between the nozzle and the collection plate, a polymer jet is developed.[5] As the charged solution is pulled electrically to the collector plate, the diameter of the jet becomes smaller because of extensional flow and evaporation until a solidified polymer fiber is deposited on the plate. Depending on the chosen electrospinning parameters and the composition of the polymer solution, the morphology of the spun polymer can result in smooth or beaded fibers.[6]

Many investigators have tried to explain the process through which fibers are created and determine the effect of electrospinning parameters on fiber morphology. Some parameters studied have been voltage, solution viscosity, solution surface tension, solution concentration, the distance between syringe needle and collection plate, temperature, solvents, and ambient humidity.[1,6–11] A number of tests have been done with voltages ranging from 5 to 30 kV and have been performed in atmospheric conditions. One characteristic behavior in fiber electrospinning is the production of a Taylor cone of solution at the tip of the nozzle. This was first described by Lord Taylor in 1969.[5]

A challenge to investigators has been to fully understand the mechanics of the electrospinning process. Some have developed analytical models to aid in this pursuit. Yarin et al.[7] proposed a mathematical model to predict how the polymer solution is pulled into a liquid jet and how the jet diameter decreases as the solution begins to spin. This model also predicts where the fiber will be placed on the collection plate by considering the forces created by the electric field and by gravitational forces. This group was also able to model the characteristic whipping of the solution jet in a circular motion as it travels to the collector plate. Tripatanasuwan

Correspondence to: C. J. Schwartz (cschwartz@tamu.edu).

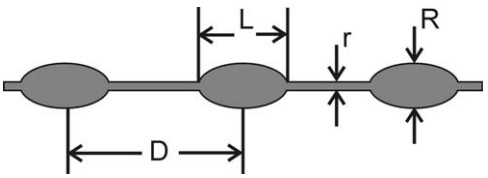

Figure 1 Illustration of fiber jet with entrained beads indicating various metrics used for characteristic dimensions.

et al.[12] went a step further in demonstrating and describing mechanistically what is happening to the jet as it travels to the plate. They showed that humidity affects the evaporation rate of the solution, leading to beads entrained in the fibers and a smaller fiber diameter between the beads. This is referred to as the capillary effect,[12] which occurs when the wavelengths of disturbances are greater than the diameter of the jet. These disturbances may be wind induced or electrical signals in the case of electrospinning polymer fibers.[11] In reaction to becoming unstable because of these disturbances, surface energy effects drive portions of the liquid jet to spherical shapes. During electrospinning, the solidification of the polymer takes place before separate spherical droplets can detach, thus resulting in a string of fibers with beaded "pearls" along the line. This is illustrated in Figure 1. Although many electrospinning parameters (voltage, weight percent, solvent, and distance traveled) have been shown to affect the fiber morphology of the electrospun polymer, there has been little substantive work to relate electrospinning to larger-scale liquid jet phenomena, specifically those that involve fluid mechanics.

In this article, the authors have focused on relating the mechanisms of fluid jet breakup to the morphology of electrospun nanofibers. Outside of the realm of electrospinning research, Lin and Reitz[11] studied the types of jet breakup that can occur when a pure fluid (water) is propelled out of a nozzle, using material properties such as viscosity, surface tension, characteristic diameter, and velocity. Lin and Reitz were able to predict the distance that a fluid jet will travel before it begins to break up into a series of droplets by calculating the Weber number of the liquid jet. The formula for determining this dimensionless quantity is as follows:

$$We = \frac{\rho U^2 d}{\sigma} \tag{1}$$

where U is the velocity of the jet, d is the characteristic diameter of the jet, ρ is the density of the solution, and σ is the surface tension of the solution. Essentially, Weber number indicates the ratio of inertial energy to surface energy in a free jet flow. It is believed to be applicable to the electrospinning process because the solution travels as a free jet to the collection plate. Many of the parameters or processing variables important in electrospinning fibers can be accounted for by the use of Weber number. The surface tension and density of a polymer solution are determined by the weight percent of dissolved polymer. The voltage and distance between nozzle and collection plate affects the diameter of the fibers created. The velocity of the jet can be controlled by the force exerted to pull the jet to the plate, which is produced by the applied voltage. In Lin and Reitz's study, Weber number was used to indicate the type of jet breakup that would occur in larger jets as the Weber number crossed threshold values. In this study, the authors characterized the velocity and diameter of the electrospun fibers under varying parameters to determine whether Weber number maintained relevance at the jet sizes produced by electrospinning. The fundamental goal of the work was to determine whether Weber number could be used to predict fiber morphology and flow characteristics.

Poly(ethylene oxide) (PEO) dissolved in water has been extensively studied for electrospinning applications because of its solubility and its various uses; however, researchers have observed that beaded morphologies commonly occur when the fraction of polymer in the solution is lowered to amounts nearing 4 wt %. In many cases, well-formed fibers are produced at higher PEO concentrations. Little explanation has been given for the sudden appearance of the entrained-bead morphology at low polymer concentrations. This article details the experimental work involved in determining the flow parameters during electrospinning as they relate to Weber number and fiber morphology to determine whether this approach can explain the appearance of the beaded morphology at low concentrations. The goal was to determine whether a threshold Weber number exists to allow fiber morphology to be predicted and controlled not only in PEO solutions, but also in other polymer systems.

EXPERIMENTAL PROCEDURE

Surface tension measurement

PEO (Sigma Aldrich, St. Louis, MO) with a molecular weight of 400,000 g/mol (M_v) was used in this study. Solutions of distilled water with between 4 and 8 wt % of PEO were prepared in the laboratory by adding PEO powder to the water and using a magnetic stir bar to completely dissolve the polymer. The solutions were then taken to a contact angle analyzer (Edmund Optics FTA188 Video Tensiometer) to measure their surface tensions.

Electrospinning

Electrospinning was performed in atmospheric conditions, and a digital thermometer was used to monitor the temperature and humidity of the ambient environment. PEO solutions were held in either a 1- or a 10-mL syringe, based on spinning rate, and placed on a syringe pump (KD Scientific 780100). The syringe was fitted with a 23-gauge needle with an outside diameter of 0.62–0.64 mm and an inner diameter of 0.32–0.34 mm. A high-voltage power supply (Glassman High Voltage, Inc., High Bridge, NJ) with a range of 0–30 kV was used to apply a potential between the syringe needle and the collector plate. A digital microscope (DinoCapture) was used to observe the electrospun jet and other phenomena during the electrospinning process. A flat copper collector plate was placed 125 mm from the needle tip and was attached to the ground source. Voltages ranging from 3.5 to 11 kV were applied to the syringe via an alligator electronic connector clamped onto the needle. A LabView program was written to control the high-voltage power supply remotely. The testing at voltages of 5 kV and below required a 5-s pulse of 11 kV to produce a Taylor cone. The voltage was then reduced to the target value for the remainder of the test. This startup procedure was needed to overcome the surface tension of the solution, which would have kept electrospinning from occurring at lower voltages. During testing at lower voltages, the rate at which the PEO solution was ejected from the syringe was set at 0.02 mL/h to ensure that Taylor cone stayed in the same conical shape throughout the test. Higher voltages, ranging from 6 to 11 kV, did not require an initial pulse; they were able to be spun immediately after the voltage was introduced. The rate at which the syringe pump was operated, for these voltages, varied between 0.2 and 1.5 mL/h to ensure the stability of the Taylor cone. All tests were run for 10–20 min. During testing, it was important to maintain steady flow conditions; this was done by making sure that none of the solution built up into large droplets on the needle and fall from the tip. This entailed several preliminary test runs of the electrospinning setup to determine the proper dispensing rate of the syringe pump. Each concentration–voltage combination for electrospinning was tested five times in a randomized sequence, and mean values were calculated for the measured parameters.

An ultrahigh-molecular-weight polyethylene film was placed in front of the copper plate to collect the fibers produced during testing. To determine the flow parameters such as flow rate and velocity, it was necessary to determine the mass of PEO deposited at the collector plate. The target polymer mass delivery rate was set using the syringe pump, and this value was corroborated by measurement of the change in syringe weight before and after the test. The PEO concentration of the solution was used to convert the syringe weight change to the mass of PEO dispensed. Measurements showed that the syringe measurement of PEO mass flow rate agreed well with the pump setting. To determine the mass of PEO reaching the target, subject to the deposition of fibers outside of the target area, the mass difference of the polyethylene film from before and after the test was measured. At various settings of voltage and solution concentration, the PEO mass measured at the target was consistently within 10% of the mass dispensed by the syringe pump. Therefore, it was decided that the change in mass of a thoroughly dried target film would be used for mass flow rate calculations. Immediately after electrospinning, the polyethylene sheet was placed on a shelf to dry for 24 h. After drying, the sheets were weighed, then sputtered coated with a gold–palladium mixture, and imaged using a JEOL 6400 scanning electron microscope (SEM).

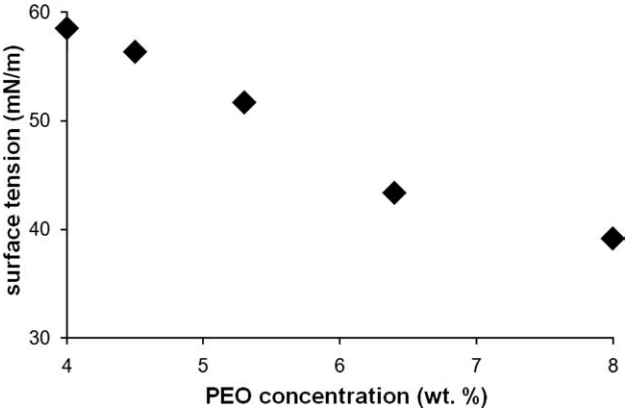

Figure 2 Plot of surface tension of various concentrations of PEO in water, showing that surface tension decreases with increasing concentration.

RESULTS

Surface tension results

The surface tension of various PEO concentrations is shown in Figure 2. It was observed that surface tension decreased as the weight percent of the solution increased. The data agree well with that of Kim et al.[13] values of surface tension of PEO solutions. The somewhat surprising result that surface tension decreases with increasing polymer concentration has been attributed to a high-concentration adsorbed film of PEO that forms on the surface of the solution, which reduces the hydrogen bond strength of the water at the surface.

TABLE I
Morphologies of Electrospun PEO Ordered by Mean Weber Number

Weight percent	Voltage (kV)	Mean fiber diameter (nm)	Mean Weber number	Morphology
4.0	4.5	150	1.8	Fibers
6.6	7.0	200	2.6	Fibers
5.3	7.0	270	6.2	Fibers
8.0	10	300	13	Fibers
6.6	10	200	13	Fibers
8.0	7.0	180	26	Fibers
5.3	10	150	39	Beaded fibers
4.0	6.8	230	40	Beaded fibers
4.0	10	350	71	Beaded fibers
4.0	11	300	86	Beaded fibers

Fiber diameter

The electrospun fibers were examined in the SEM to get a detailed look at the resultant fiber morphology and to measure fiber diameters. The accelerating voltage for the SEM was set to 15 kV with a working distance of 15 mm. High-magnification images were taken to measure the diameter of the electrospun material. Because fiber diameter was used to determine the jet velocity (through a mass flow rate relation), the presence of entrained beads required a technique that accounted for a representative material volume to be consistent with the nonbeaded fibers. Measurement approaches that focused on either the thin fibers or the beads alone suffered from shortcomings. The diameter of fibers connecting two beads was very small, which would lead to artificially high calculated velocities. On the other hand, using the maximum diameter of the beads themselves would underestimate jet velocity. It was decided to use a weighted average diameter, which incorporated the diameters of both the connecting fibers and the beads in such a way as to maintain consistency across the various samples with entrained beads. Electrospun material that had entrained beads had connecting fiber diameters in the range of 80–150 nm, and the beads themselves had diameters in the range of 400 nm to 1.00 μm. An average diameter of the resultant beaded fiber was calculated to effectively handle the varying diameter because of the entrained beads. By using the SEM images, a weighted average of fiber–bead diameter was calculated by measuring the ratio of connector fiber and bead lengths and assigning a corresponding weight to the diameter measurements. Mean diameters of the beaded fibers were in the range of 280–350 nm in size, larger than the size of the fiber but smaller then the size of the beads.

Weber number

Mass flow rate was calculated by dividing the mass of PEO deposited onto the polyethylene film by the length of time the test was run. From mass flow rate, volume flow rate was calculated by dividing the mass flow rate by the calculated density of the polymer solution. The velocity of the jet (U) was calculated by dividing the volume flow rate with the area of the jet before it reached the collection plate. In this study, the diameter of the jet near at the plate was assumed to closely approximate the diameter of the resultant fiber deposited at the target, which was imaged in the SEM. The measured diameter, as described above, was used to calculate the area of the jet. There is likely some reduction in fiber diameter as solvent evaporates from the jet after leaving the syringe; however, the direct measurement of this "wet" diameter is intractable with the current approach. To address this issue, the authors decided that the final diameter of a dried fiber provides a reasonable estimate of the wet fiber diameter, and, furthermore, dry fibers diameters will follow the same trend as wet fibers with respect to the parameters studied here. It was assumed that the liquid jet was cylindrical in shape as it traveled to the plate. Once velocity of the jet was obtained, Weber number was calculated based on.[1]

Table I reports the morphology results ordered by calculated mean Weber number. In cases when the PEO material was spun into fibers with no beads present, the Weber number ranged from 0.12 to approximately 20, with velocities of the jet ranging from 15 to 50 m/s. The SEM images in Figures 3–5 show different weight percents of PEO solution electrospun at different voltages, resulting in various fiber morphologies. In cases where the calculated Weber number was greater than approximately 40, morphologies with many entrained beads were observed. The velocities in these cases were calculated to be above 50 m/s. The results shown in the table clearly suggest that there is a transition from pure fibers to entrained beaded-fibers based on a Weber number threshold. It may be argued that this transition occurs somewhere between the Weber number values of 26 and 39.

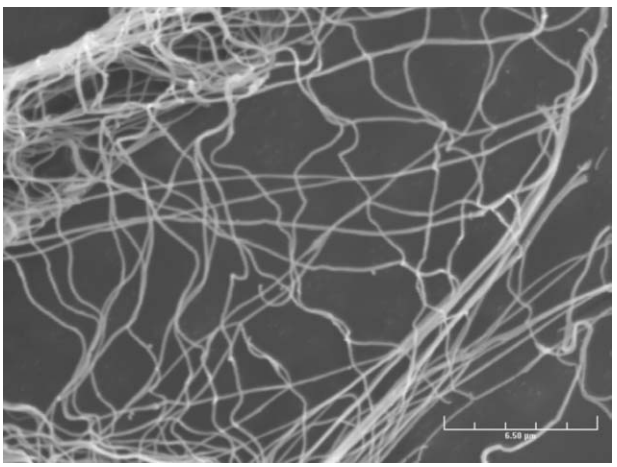

Figure 3 Nonbeaded electrospun fibers produced with 4.5 kV voltage and 4 wt % PEO solution.

DISCUSSION

Surface tension

The surface tension of the PEO solution decreased with the increase in weight percent of PEO. Although this may seem somewhat counterintuitive, this behavior has been demonstrated previously.[9] The drop in surface tension is due to the hydrophobic nature of the CH_2CH_2 segments of the PEO backbone (—CH_2CH_2O—). As the concentration of the polymer increases, the resulting solution becomes less and less hydrophilic.[13] As is currently hypothesized in this work, Weber number is a strong indicator of electrospun fiber morphology. Because the surface tension term is so prominent in the calculation of this dimensionless parameter, it becomes vital to understand the surface tension behavior of PEO and other polymer solutions. Most polymers in a solvent approach a critical concentration past which further polymer does not dissolve.[13] Therefore, the control of nanofibers morphology by using Weber number must take into account the ability to change the surface tension of various polymer solutions.

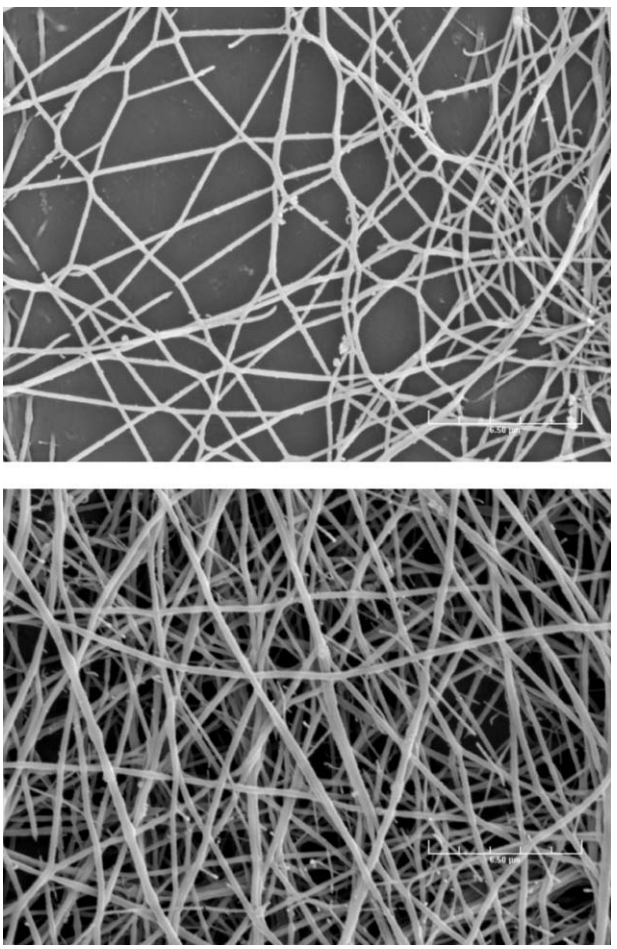

Figure 4 Electrospinning results for 5.3 and 8 wt % PEO solution electrospun at (a) 5.3 wt % and 7 kV and (b) 8 wt % and 10 kV.

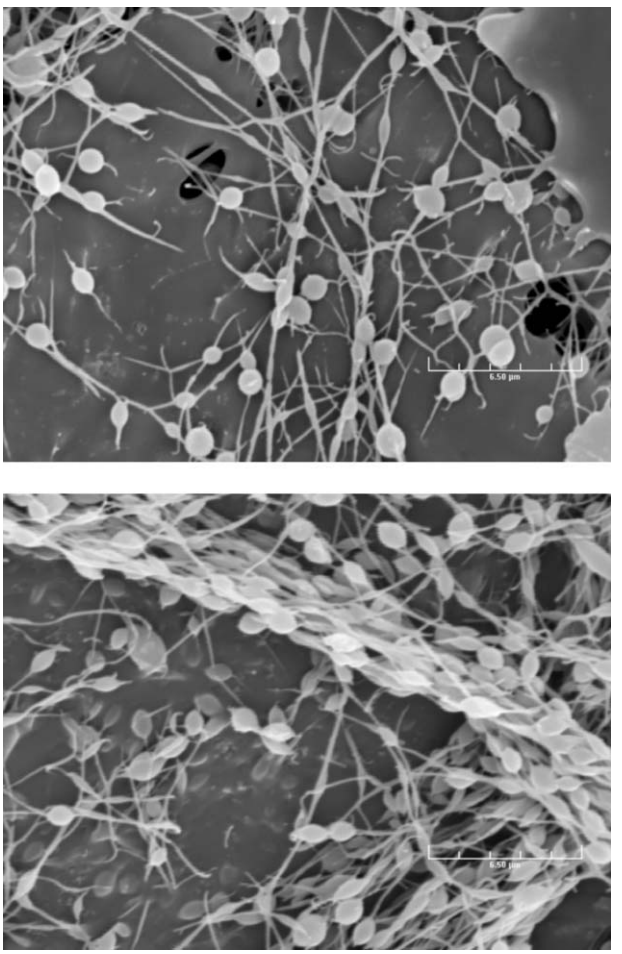

Figure 5 Electrospinning results of 4 wt % PEO solution spun at (a) 11 kV and (b) 6.8 kV, respectively, showing entrained beads in contrast to 4 wt % fibers spun at 4.5 kV (see Fig. 3).

Weber number

These results show that the Weber number can be used as an indicator of fiber morphology. Examination of Table I and Figures 3–5 shows that there is

a clear distinction in the Weber numbers that correspond to nonbeaded and beaded morphologies. When Weber number exceeds approximately 40, all of the tests produced fibers with entrained beads. An informative exercise is to examine all of the 4 wt % PEO solutions studied. Previous researchers have reported the presence of entrained beads at low solution concentrations,[6,9] and the same was observed during this study at voltage settings in the same range as higher-concentration solutions. However, the viscosity of the lower-concentration solution is low, and, thus, the extensional flow behavior of the electrospun jet allows for higher flow velocities and, thus, higher Weber number values as shown in the table. When the voltage is reduced to reduce the flow velocity, entrained beads are no longer present and Weber number values are correspondingly low. This same behavior was reproduced with a 5.3 wt % solution as shown in the table. The prediction and eventual control of fiber morphology based on Weber number must take into account the process parameters that are controllable in a given electrospinning setup. In this case, the two directly controllable parameters were applied voltage and PEO concentration. An effect on all of the terms of Weber number could be observed from manipulation of these two parameters. Changing PEO concentration affected the density and surface tension of the solution, whereas applied voltage affected the velocity of the jet. Furthermore, although not reported here, variation of PEO concentration affected extensional viscosity of the jet and, thus, greatly affected the resulting fiber diameter. The manipulation of these two process parameters, polymer concentration and applied voltage, is in line with other researchers working on the electrospinning of polymer fibers.

As stated above, Weber number brings together various fluid and process characteristics and incorporates them into one dimensionless number. It is envisioned that Weber number analysis could be applied to other polymer–solvent systems to control the nanofiber morphology. The transition range identified in this work for aqueous solutions of PEO, between 26 and 39, may not be the same for every polymer–solvent system tested, but this work shows that the concept of using Weber number to describe the free jet flow of electrospun fibers is valid. It follows that a transition range will exist in other systems such that Weber number values below the transition will result in fibers, whereas values above the transition will result in entrained beads. Future work is needed to identify the numerical values of these transitions in other polymer solutions.

The Weber transition range identified in this study differs from Lin and Reitz's[11] values for the first stage of fluid jet breakup, above approximately 45. The four stages of jet breakup in Lin and Reitz's study include Rayleigh breakup, first wind induced, second wind induced, and atomization. It is hypothesized because of the resulting morphologies and calculated Weber numbers that this work involved only Rayleigh breakup of the jet. Further study would be needed to determine whether the PEO solution is capable of other types of breakup, thus making additional morphology options available such as ultrafine electrospun beads.

CONCLUSIONS

The following conclusions are made based on the results of this work:

1. Two fiber morphologies were observed in the electrospinning of PEO solution, pure fibers and fibers with entrained beads. The appearance of entrained beads was due to a mechanism of fluid-jet breakup.
2. Weber number is an appropriate gauge of the free-jet flow conditions of the electrospun jet and, thus, can indicate the conditions that lead to the two morphology types. At Weber numbers below approximately 26, nonbeaded fibers result, whereas at values above 39, entrained beads are produced. Further investigation is needed to obtain more precision in this number and to determine how sharply behavior transitions from nonbeaded to beaded fiber morphologies.
3. The Weber number values that indicate a transition from nonbeaded to beaded fibers agree reasonably well with work done in the jet breakup of pure liquids. This signifies that fundamental free-jet breakup mechanics can describe the electrospinning process well.

The authors thank the Microscopy Center at Texas A&M University for use of the SEM and Mr. Kevin Plumlee for consultation and editing assistance.

References

1. Zeng, J.; Xu, X.; Chen, X.; Liang, Q.; Bian, X.; Yang, L.; Jing, X. J Control Release 2003, 92, 227.
2. Zhang, Y.-J.; Huang, Y.-D.; Wang, L.; Li, F.-F.; Gong, G.-F. Mater Chem Phys 2005, 91, 217.
3. Sawicka, K.; Gouma, P. J Nanoparticle Res 2006, 8, 769.
4. Yeo, L. Y.; Friend, J. R. J Exp Nanosci 2006, 1, 177.
5. Taylor, G. Proc Roy Soc Lond Math Phys Sci 1969, 313, 453.
6. Fong, H.; Chun, I.; Reneker, D. H. Polymer 1999, 40, 4585.
7. Yarin, A. L.; Koombhongse, S.; Reneker, D. H. J Appl Phys 2001, 89, 3018.
8. Yarin, A. L.; Kataphinan, W.; Reneker, D. H. J Appl Phys 2005, 98, 064501.
9. Deitzel, J. M.; Kleinmeyer, J. D.; Hirvonen, J. K.; Beck Tan, N. C. Polymer 2001, 42, 8163.
10. Casper, C. L.; Stephens, J. S.; Tassi, N. G.; Chase, D. B.; Rabolt, J. F. Macromolecules 2004, 37, 573.
11. Lin, S. P.; Reitz, R. D. Annu Rev Fluid Mech 1998, 30, 85.
12. Tripatanasuwan, S.; Zhong, Z.; Reneker, D. H. Polymer 2007, 48, 5742.
13. Kim, M. W.; Cao, B. H. Europhys Lett 1993, 24, 229.